AUTHOR	Li Lili, Zhou Ping, Wang Yidi, Pan Ying, Chen Min, Tian Ye, Zhou Hua, Yang Baoru, Meng Hecheng, Zheng Jie
TITLE	Antimicrobial activity of cyanidin-3-O-glucoside–lauric acid ester against Staphylococcus aureus and Escherichia coli
YEAR	2022
DOI	https://doi.org/10.1016/j.foodchem.2022.132410
VERSION	Author's accepted manuscript
COPYRIGHT	License: CC BY NC ND
CITATION	Lili Li, Ping Zhou, Yidi Wang, Ying Pan, Min Chen, Ye Tian, Hua Zhou, Baoru Yang, Hecheng Meng, Jie Zheng, Antimicrobial activity of cyanidin-3-O-glucoside–lauric acid ester against Staphylococcus aureus and Escherichia coli, Food Chemistry, Volume 383, 2022, 132410, ISSN 0308-8146, https://doi.org/10.1016/j.foodchem.2022.132410.

Antimicrobial activity of cyanidin-3-*O*-glucoside–lauric acid ester against *Staphylococcus aureus* and *Escherichia coli*

Lili Li[a], Ping Zhou[b, c], Yidi Wang[d], Ying Pan[e], Min Chen[b], Ye Tian[f], Hua Zhou[b], Baoru Yang[f], Hecheng Meng[d], Jie Zheng[*,b,g]

[a] Institute of Food Safety and Nutrition, Jinan University, Guangzhou 510632, Guangdong, China

[b] Department of Food Science and Engineering, Jinan University, Guangzhou 510632, Guangdong, China

[c] InnoStar Bio-Tech Nantong Site, Nantong 226133, Jiangsu, China

[d] School of Food Science and Engineering, South China University of Technology, Guangzhou 510641, Guangdong, China

[e] Department of Obstetrics and Gynecology, the First Affiliated Hospital of Jinan University, Guangzhou 510632, Guangdong, China

[f] Food Chemistry and Food Development Unit, Department of Life Technologies, University of Turku, Turku FI-20014, Finland

[g] Zhongshan Hongli Health Food Industry Research Institute Co., Ltd, Zhongshan 528400, Guangdong, China

*Corresponding Author

Jie Zheng: ORCID 0000-0001-9755-5595

Department of Food Science and Engineering, Jinan University, Guangzhou 510632, Guangdong, China

E-mail address: zhengjie@jnu.edu.cn

ABSTRACT

Enzymatic acylation of anthocyanin with fatty acid improves its lipophilic solubility and application potential. Nevertheless, evaluation of functional properties of product is premise for application. This study investigated the antimicrobial potential and the underlying mechanisms of an acylated anthocyanin, namely, cyanidin-3-*O*-glucoside–lauric acid ester (C3G–LA), to provide guidelines for its application. C3G–LA exhibited outstanding antibacterial activity against *Staphylococcus aureus* [minimum inhibitory concentration (MIC) = 0.3125 mg/mL] and modest activity against *Escherichia coli* (MIC = 5 mg/mL). Moreover, C3G–LA manifested bactericide ability against *S. aureus* at 0.625 mg/mL. Decreases in membrane integrity (by 96% and 92% at MIC in *S. aureus* and *E. coli*, respectively), intracellular ATP concentration (by 96% and 92%) and intracellular pH (by 11% and 9%) and changes in cellular morphology altogether indicated the dysfunction of cell membrane under C3G–LA treatment. These findings demonstrated that C3G–LA could be adopted as an alternative food preservative against foodborne pathogens.

KEYWORDS: anthocyanin, acylation, cyanidin-3-*O*-glucoside–lauric acid ester, *Staphylococcus aureus*, *Escherichia coli*, antimicrobial activity

1. INTRODUCTION

Anthocyanins are water-soluble phenolic compounds that are ubiquitously distributed in nature, especially in fruits and vegetables (Liu et al., 2020). Apart from their native role as natural pigments for providing attractive colours to flowers, fruits and vegetables, their effects on human health have been widely examined in recent years given their abundance in different food types, hence the high dietary intake (Aloud et al., 2020). Multifarious bioactivities and functions have been reported about anthocyanins. For instences, anthocyanins have antioxidant, anti-hyperglycaemic, anti-hyperlipidemic and anti-inflammatory activities (Chen et al., 2019; Jugran, Rawat, Devkota, Bhatt, & Rawal, 2021). These activities support the prevention and treatment of various chronic diseases, such as diabetes (Chen et al., 2020), cardiovascular diseases (Krga & Milenkovic, 2019), hypertension (Aloud et al., 2020), osteoarthritis (Jiang et al., 2019), cognitive dysfunction (Wei et al., 2017), Alzheimer's disease (Liu et al., 2020) and cancer (Wang et al., 2019). Therefore, anthocyanins have been popularly applied as functional ingredients in the food, cosmetics, nutraceutical and pharmaceutical industries. However, anthocyanins also have many drawbacks, such as apparent sensitivity to temperature and light and low solubility in lipophilic media, largely limiting their application.

In view of overcoming the aforementioned drawbacks, lipophilization via enzymatic acylation has become a theoretically promising process and it is widely investigated in the last decades as a means of extending the application of anthocyanins (Marquez-Rodriguez et al., 2021). As a result, anthocyanins obtained from various herbs, flowers and fruits and even industrial wastes, such as malvidin-3-*O*-glucoside (Cruz et al., 2017), cyanidin-3-*O*-glucoside (C3G) (Guimarães, Mateus, de Freitas, & Cruz, 2018), cyanidin-3-*O*-galactoside

(Yang, Kortesniemi, Yang, & Zheng, 2018), cyanidin-3-*O*-rutinoside, delphinidin-3-*O*-rutinoside, delphinidin-3-*O*-glucoside (Yang, Kortesniemi, Ma, Zheng, & Yang, 2019) and delphinidin-3-*O*-sambubioside (Marquez-Rodriguez et al., 2021), have been successfully esterified with fatty acids of different chain lengths. The evaluation of acute, subacute and sub-chronic toxicities of anthocyanin–lauric acid derivatives suggested that they are nontoxic agents (Yang et al., 2020a). The 50% lethal dose (LD_{50}) of anthocyanin–lauric acid derivatives was > 10 g/kg body weight (BW) in mice. Moreover, no adverse effects were observed at the oral administration level of 2.50 g/kg BW in the subacute toxicity test and 0.60 g/kg BW in the sub-chronic toxicity test (Yang et al., 2020a). Meanwhile, acylated anthocyanins also demonstrated improved lipophilicity, stability and antioxidant capacities (Marquez-Rodriguez et al., 2021; Guimarães et al., 2018; Zhang et al., 2021). C3G is a major anthocyanin in legumes, black rice, purple potato and black beans (Zhang et al., 2021). Owing to the wide distribution of C3G in nature, it is one of the most investigated anthocyanins. Cyanidin-3-*O*-glucoside–lauric acid ester (C3G–LA) displayed significantly better thermostability, photostability, pH resistivity and *in-vivo* cellular antioxidant capacity than C3G; it also promoted the proliferation of intestinal probiotics *Bifidobacteria* and *Lactobacillus* (Yang et al., 2020b; Zhang et al., 2021). However, the application properties of anthocyanin esters are far from being fully explored.

Foodborne pathogens, such as *Staphylococcus aureus* (*S. aureus*), *Escherichia coli* (*E. coli*), *Listeria monocytogenes* and *Salmonella*, have caused numerous gastroenteritis and food-poisoning incidents and other associated diseases annually, and they contribute to huge economic losses worldwide. The use of preservatives provides effective solutions by inhibiting the growth of food pathogens and prolonging the shelf life of food. However, consumers tend to be anxious toward the potentially negative health effects of synthetic preservatives and the continuously increasing antimicrobial-resistant bacterial strains. Natural food-derived ingredients, such as anthocyanin, organic acids and plant essential oils, are expected to serve as potential preservatives for the inhibition of food pathogens (Gong et al., 2021). Researchers have reported that anthocyanins have antibacterial properties (Gong et al., 2021) and suggested their application as antibacterial materials in food production.

This study evaluated the antibacterial activity of C3G–LA against two most investigated food pathogens, i.e. *S. aureus* and *E. coli*, to demonstrate whether adding fatty acid moiety could improve the antibacterial potential of anthocyanins by elevating their lipophilicity. Cell damage, bacterial membrane integrity, intracellular ATP production and intracellular pH (pH_{in}) were investigated to elucidate the interactions between C3G–LA and the abovementioned two food pathogens. This study aimed to gather insights by exploring the application of the newly derived lipophilic anthocyanin–fatty acid ester.

2. MATERIALS AND METHODS

2.1 Reagents and bacterial strains

Anthocyanin extracts from black bean hulls were provided by BGG Co., Ltd (Beijing, China). Lauric acid, standard of C3G and molecular sieves (4 Å) were purchased from Energy Chemical (Shanghai, China). Novozyme 435 (*Candida antarctica* lipase B) was purchased from Jian Quan Biological Technology Co., Ltd (Sichuan, China). The *S. aureus* and *E. coli* strains were laboratory-stored strains routinely grown in brain–heart–extract (BHI) broth and Luria–Bertani (LB) broth or agar plates at 37 °C for 18 h, respectively.

All growth media were obtained from Guangdong Huankai Biotechnology Co., Ltd (Guangzhou, China). All reagents and antibiotics were purchased from Shanghai MacLean Biochemical Technology Co., Ltd (Shanghai, China).

2.2 Preparation and characterisation of C3G–LA

A preparation method developed by the authors' laboratory (Zhou et al., 2021) was applied to directly achieve C3G–LA from the black bean hull crude extract containing 35.8% C3G. No anthocyanin purification was required prior to the esterification reactions. The black bean hull crude extract (3 g) and lauric acid were dissolved in a mixture of 5 mL dimethylformamide (DMF) and 45 mL *tert*-butanol. The *tert*-butanol was pre-dried overnight with 4 Å molecular sieves (100 g/L) before use. The molar ratio of C3G to lauric acid was 1:10. The reaction started with the addition of 0.5 g Novozyme 435 and continued at 60 °C for 72 h with continuous magnetic stirring. As esterification may be hindered by water generation, molecular sieves (4 Å, 100 mg/mL) were applied to maintain a low water activity throughout the reaction. The reaction was stopped in accordance with the filtration of the molecular sieves and the enzyme. The reaction mixture was evaporated using a vacuum to remove the *tert*-butanol. The residues were dissolved in a mixture of NaCl-saturated solution (20 mL), $NaHCO_3$-saturated solution (20 mL) and ethyl acetate (50 mL). The C3G–LA specimen was collected in the ethyl acetate phase via liquid−liquid extraction. An adequate volume of ethyl acetate was applied until the extraction fraction turned colourless. All of the extracts were combined and ethyl acetate was removed using a rotary evaporator. The ester extract was then further purified on a chromatographic column filled with silica via successive elution with dichloromethane/methanol/formic acid at 20:1:1, 15:1:1, 13:1:1 and 10:1:1 (v/v/v). The fraction that comprised C3G–LA with purity over 95% was collected, dried under reduced vacuum and kept at –20 °C for further use.

The purity of the acylated product was analysed using a Shimadzu LC-20AT HPLC–DAD system (Shimadzu Corporation, Kyoto, Japan) accompanied with an Aeris peptide XB-C18 (4.60 × 250 mm, 5 μm) column (Phenomenex, Torrance, CA, USA). The binary gradient programme with 5% formic acid in water (solvent A) and acetonitrile (solvent B) was applied as follows: 0–5 min, 5%–10% B; 5–10 min, 10% B; 10–20 min, 10%–30%B; 20–30 min, 30%–90% B; 30–33 min, 90% B; 33–35 min, 90%–5% B; and 35–45 min, 5% B. The total flow rate was 0.5 mL/min and the injection volume was 10 μL. The peak areas of the anthocyanin and its derivative were recorded at 520 nm and the concentrations were quantified with the corresponding standards. The acylation rate of the C3G specimen was calculated as the percentage of the molar concentration of C3G–LA in the initial molar concentration of C3G.

Highly purified C3G–LA was dissolved in CD_3OD:CF_3COOD (95:5, v/v) and characterised by ^{1}H and ^{13}C nuclear magnetic resonance (NMR) analysis with an Avance III HD 600 NMR spectrometer (Bruker, Fällanden, Switzerland). The ^{1}H NMR data were recorded as follows: chemical shift [δ, ppm; multiplicity, coupling constant(s) J (Hz), relative integral].

2.3 Antibacterial activity assessment

The minimum inhibitory concentration (MIC) values of C3G and C3G–LA were determined via broth microdilution method (CLSI, 2017). Briefly, the *S. aureus* and *E. coli* strains were grown aerobically overnight at 37 °C on BHI and LB agar, respectively. The colonies were suspended in 0.9% NaCl and adjusted to 0.5 McFarland standard with a Sensititre nephelometer (Thermo-Fisher Scientific, Eugene, Oregon, USA). Subsequently, the suspensions were 100-fold diluted in Mueller–Hinton broth (MHB) and 100 μL of the dilution was transferred to the wells of a sterile 96-well plate added with different concentrations of C3G–LA or C3G in MHB (100 μL). The final concentrations ranged from 0.02 mg/mL to 10 mg/mL. The positive controls contained bacteria inoculum only, whereas the negative controls contained MHB only. The lowest concentration of the compounds that resulted in no visible growth of test organisms was determined as the MIC. The MIC values were determined in biological triplicates.

2.4 Growth and viability assays

Growth and viability assays were performed as previously described with minor modifications (Ronco et al., 2020). Briefly, *S. aureus* ATCC 25923 and *E. coli* ATCC 25922 were applied as test strains and the assay was prepared under 37 °C for 12 h with continuous shaking. The strains were grown overnight and re-suspended in BHI broth to reach OD_{600} = 0.1 and then exposed to 0, 1/2× MIC, MIC and 2× MIC of C3G and C3G–LA. The samples (100 μL) were collected at seven different time points during the 12-h period. Then, they were serially diluted, spread on Mueller−Hinton agar (MHA) plates and incubated at 37 °C for 18 h, followed by successive counting. The experiment was performed in triplicate and the result was expressed as the average $Log_{10}CFU/mL$.

2.5 Assessment of membrane integrity

The influence of C3G and C3G–LA treatments on the membrane integrity of *S. aureus* ATCC 25923 and *E. coli* ATCC 25922 was assessed using the LIVE/DEADTM *Bac*Light Bacterial Vitality Kit (Thermo-Fisher Scientific, Eugene, Oregon, USA), as previously reported (Alakomi, Mättö, Virkajärvi, & Saarela, 2005). Briefly, standard samples were firstly prepared to construct a standard curve. The results depicted by the standard curves illustrated a good linear relationship (R^2 = 0.99) between the green fluorescence intensity at 530 nm and the percentage of viable bacteria of *E. coli* 25922 and *S. aureus* 25923 (Fig. S1). The strain cultures were grown to the late exponential phase and they were centrifuged, washed two times and re-suspended in 0.85% NaCl or 70% isopropyl alcohol (for the killed bacteria). Then, the suspensions were incubated at room temperature for 1 h with mixing every 15 min. After incubation, the samples were pelleted two times by centrifugation at 10,000 g for 10 min and re-suspended in NaCl to reach OD_{600} = 0.5. Different viable cell proportions (0, 10%, 50%, 90% and 100%) were utilised as the standard samples. A working stain solution (2×) was prepared by adding 6 μL of SYTO 9 and 6 μL of propidium iodide (PI) to 2 mL of filter-sterilised water.

The culture strained overnight was adjusted to OD_{600} = 0.5, followed by treatment with C3G or C3G–LA at 0, 1/2× MIC, MIC and 2× MIC for 15 min at 37 °C. After the treatment, the culture was centrifuged and re-suspended in 0.85% NaCl. Then, an equal volume of 100 μL cell suspension and working stain solution (2×) were added to black opaque 96-well microtitration plates (Corning, New York, USA) and mixed thoroughly. The mixture was cultured in darkness at 25 °C for 15 min. Fluorescence was determined using a multifunctional enzyme marker (BioTek, Vermont, USA). The green (530 nm) and red (630 nm) emission integral intensities of the suspension excited at 485 nm were obtained three times via wavelength measurement.

2.6 Measurement of intracellular ATP concentrations

The influence of C3G and C3G–LA on the intracellular ATP concentrations of *S. aureus* ATCC 25923 and *E. coli* ATCC 25922 was assessed in accordance with a method described previously (Sánchez, García & Heredia, 2010). Briefly, the strains cultured overnight were harvested by centrifugation (5000× g, 5 min). Then, the cells were washed three times with 0.1 mol/L phosphate-buffered saline (PBS, pH 7.0) and re-suspended in PBS to achieve OD_{600} = 0.5. Subsequently, C3G and C3G–LA were added to each tube to achieve the final concentrations of 0, 1/2× MIC, MIC and 2× MIC and cultured at 37 °C for 30 min. The ATP was ultrasonically extracted on ice and centrifuged (5000× g, 5 min). The supernatant was kept on ice to avoid ATP loss. The ATP content was determined using an ATP Assay Kit (Beyotime Biotechnology, Shanghai, China) with a multifunctional enzyme marker (BioTek, Vermont, USA) following the manual's instructions. A good linearity was found between intracellular ATP content and luminescence (R^2 = 0.99, Fig. S2).

2.7 Measurement of pH_{in}

The influence of C3G and C3G–LA on the pH_{in} of *S. aureus* ATCC 25923 and *E. coli* ATCC 25922 was determined in accordance with a modified method of Breeuwer, Drocourt, Rombouts, & Abee (1996). Firstly, the calibration curve was constructed by measuring a series of fluorescence intensities of the pH buffers, with values in the range of 3–10. The buffers consisted of 50 mmol/L KCl, 50 mmol/L $Na_2HPO_4·2H_2O$, 50 mmol/L glycine and 50 mmol/L citric acid and they were adjusted with either NaOH or HCl. The pH_{in} and pH_{out} were equilibrated by adding 10 μmol/L valinomycin and 10 μmol/L nigericin.

Three hundred microliters of the overnight-cultured strains were transferred into 30 mL BHI broth and cultured at 37 °C for 8 h. After centrifugation (5000× g, 10 min), the cells were washed two times with 50 mmol/L HEPES buffer [containing 5 mmol/L ethylene diamine tetraacetic acid, pH = 8] and re-suspended in 20 mL buffer. Then, 3 μmol/L of the probe (carboxyfluorescein diacetate succinimidyl ester; cFDA-SE) (Meilunbio, Dalian, China) was added and cultured at 37 °C for 20 min. The cells were subsequently washed with 50 mmol/L potassium phosphate buffer added with 10 mmol/L $MgCl_2$ (pH = 7.0), re-suspended in 10 mL buffer and subsequently added with 10 mmol/L glucose and cultured at 37 °C for 30 min to eliminate the unbound cFDA-SE. The obtained particles were washed two times by using the abovementioned method and suspended in 50 mmol/L potassium phosphate buffer on ice. C3G and C3G–LA were added to the treated cell suspension to obtain the final concentrations of 0, 1/2× MIC, MIC and 2× MIC. Then, the mixture was transferred into a black opaque 96-well microtiter plate. After treatment for 20 min, fluorescence intensity was measured under the excitation wavelengths of 440 and 490 nm, with an emission wavelength of 520 nm, at 25 °C by using a multifunctional enzyme marker (BioTek, Vermont, USA). The pH_{in} was determined as the ratio of fluorescence signals at the pH sensitive wavelength of 490 nm and pH insensitive wavelength of 440 nm. The fluorescence of the cell-free controls was measured and deducted from the fluorescence of the samples.

2.8 Field emission scanning electron microscopic (FESEM) analysis

FESEM assays were prepared as previously reported, with minor modifications (Li, Wang, Xu, Zhang, & Xia, 2014). Briefly, the cells (OD_{600} = 0.5) were treated with C3G and C3G–LA at 0, 1/2× MIC, MIC and 2× MIC and then cultured at 37 °C for 4 h. The cultured cells were centrifuged (5000× g, 10 min), washed two times with 0.85% NaCl and re-suspended in 2.5% glutaraldehyde solution and cultured at −4 °C for 10 h for fixation. Then, the cells were centrifuged (5000× g, 10 min) and dehydrated in gradient concentrations of ethanol (30%, 50%, 70%, 80%, 90% and 100%). Finally, the samples were fixed onto the FESEM support, sputter-coated with gold under vacuum and examined using a FESEM apparatus (Bruker, Berlin, Germany).

2.9 Statistical analysis

All experiments were conducted in triplicate. Statistical analyses were performed in GraphPad Prism ver. 8.0.1 (San Diego, CA, USA). Data were presented as mean ± standard deviation (n = 3) and differences between mean values were tested via one-way ANOVA. Differences were compared at confidence levels of $P < 0.05$, 0.01, 0.001 and 0.0001.

3. RESULTS AND DISCUSSION

3.1 Preparation and characterisation of acylated anthocyanin

The acylated C3G derived from black bean hulls in this study was obtained via esterification with lauric acid. The NMR analyses showed ^{1}H NMR chemical shifts of the product as follows: δ 8.90 (s, 1H, H-4), 8.24 (dd, *J* = 9.0 and 2.4 Hz, 1H, H-6′), 8.00 (d, *J* = 2.4 Hz, 1H, H-2′), 7.01 (d, *J* = 8.7 Hz, 1H, H-5′), 6.88 (dd, *J* = 5.5 and 1.1 Hz, 1H, H-8), 6.65 (d, *J* = 1.5 Hz, 1H, H-6), 5.29 (d, *J* = 7.8 Hz, 1H, H-1″), 4.43 (dd, *J* = 12.0 and 1.8 Hz, 1H, H-6″a), 4.19 (dd, *J* = 12.0 and 7.2 Hz, 1H, H-6″b), 3.76 (t/s, *J* = 6.6 Hz, 1H, H-5″), 3.66 (t, *J* = 8.4 Hz, 1H, H-2″), 3.53 (t, *J* = 9.3 Hz, 1H, H-3″), 3.39 (t, *J* = 9.3 Hz, 1H, H-4″), 2.27 (td, *J* = 7.2 and 3 Hz, 2H, –C$\underline{H}_2$–CO–), 1.46 (m, 2H, –C$\underline{H}_2$–CH_2–CO–), 1.04-1.34 (m, 16H, –CH_2–lauroyl backbone) and 0.84 (t, *J* = 7.5 Hz, 3H, –CH_3). Meanwhile, the ^{13}C NMR chemical shifts of the product were as follows: δ 174.03 (C=O), 169.07 (C7), 163.10 (C2), 157.72 (C9)， 156.25(C5), 154.66(C3), 146.15(C3′), 144.06(C4′), 135.1(C4), 129.43(C6′), 127.07(C1′), 119.76(C10), 116.98(C2′), 116.02(C5′), 102.02(C6), 101.97(C1″), 93.79(C8), 76.42(C5″), 74.58 (C3″), 73.21(C2″), 70.03 (C4″), 63.15 (C6″), 33.42 (–$\underline{C}H_2$–CO–), 22.29-31.63 (–CH_2–lauroyl backbone) and 12.98 (–CH_3). The corresponding acylation of the lauric acid was found at 6″-OH of the glucoside, yielding the product cyanidin-3-(6″-dodecanoyl)-glucoside, as reported in the previous study (Yang et al., 2019).

By introducing DMF as the cosolvent in the reaction media, the acylated anthocyanin could be directly synthesised from a crude anthocyanin extract with low purity (35.8% of anthocyanin). The acylation rate reached the highest value at 66.59% under the applied optimised conditions but the procedure could be simplified by omitting the time-consuming purification process that usually requires a high equipment cost (Zhou et al., 2021). This modified method may further facilitate the preparation and application of acylated anthocyanins in the industrial scale.

The product, cyanidin-3-(6″-dodecanoyl)-glucoside, was previously evaluated and it demonstrated improved liposolubility, antioxidant activity, thermostability, photostability, pH resistivity and probiotic activity (Yang et al., 2019; Yang et al., 2020b; Zhang et al., 2021), together with low toxicity (Yang et al., 2020a). However, its antimicrobial behaviour is rarely investigated. Thus, the antibacterial activity and the underlying mechanisms of the derived product against the most prevalent food pathogens (*S. aureus* and *E. coli*) were investigated in the present study.

3.2 Antibacterial activity of C3G–LA against *S. aureus* and *E. coli*

S. aureus, a Gram-positive food-borne pathogenic bacterium, is widely spread by air, dust, hands, sneezing and food contact surfaces and thus found in a wide range of food types and the environment (Gong et al., 2021). *S. aureus* is the second most common cause of bloodstream infection, with incidence rates of 15–40 per 100,000 population per year and case fatality rates between 15% and 25% (Laupland, Steele, Pasquill, & Parfitt, 2021). It is also a leading cause of endocardium, osteoarticular, pleuropulmonary and skin and soft-tissue infections (Tong, Davis, Eichenberger, Holland, & Fowler, 2015). *E. coli* is a Gram-negative bacterium that belongs to the family of *Enterobacteriaceae* (Jiang et al., 2017). It commonly resides in the lower intestinal tract of warm-blooded animals, including humans, and it is widely distributed in the environment through the discharge of faeces and wastewater treatment plants (Abebe, Gugsa, & Ahmed, 2020; Sarowska et al., 2019). The pathogenic strains of *E. coli* caused various human diseases and resulted in more than 1 million deaths per year (Khalil et al., 2018). The two bacterial species mentioned above are the most representative foodborne pathogens that are widely investigated with respect to the exploration of potential antimicrobial agents.

The MIC values of C3G–LA against five *S. aureus* strains and five *E. coli* strains were determined and then compared with those of C3G. The details are listed in Table 1. The MICs of C3G against all of the *S. aureus* and *E. coli* strains were at the value of 5 mg/mL. This finding is consistent with the results reported by Gong et al. (2021), who showed that cranberry anthocyanin could inhibit the growth of *S. aureus*, with an MIC value of 5 mg/mL. The MIC values of anthocyanin extracts from various blueberry cultivars against *E. coli* ranged from 20 mg/mL to 35 mg/mL (Pertuzatti, Barcia, Portugal, Rebello, & Hermosín-Gutiérrez, 2016). Anthocyanin extracts from various other sources exhibited MIC values against *E. coli* in a range of 10–400 mg/mL (Ma, Ding, Fei, Liu, Jang, & Fang, 2019). Here, C3G–LA had a stronger antibacterial activity against the *S. aureus* strains than C3G, with an MIC value of 0.3125 mg/mL, which is a 16-fold lower value. The inhibitory effect of C3G–LA on the growth of *E. coli* strains was not necessarily better than that of C3G as both specimens showed the same MIC value of 5 mg/mL (Table 1). This finding is consistent with that of Oliveira, Correia, Bessa, Guimares, & Fernandes (2021), who revealed that C3G–LA did not inhibit *E. coli* growth at the level over 0.512 mg/mL. They also reported that C3G–LA hardly inhibited the growth of *S. aureus* at levels over 0.512 mg/mL, different from the finding of the present study. Nevertheless, the trains used in the two studies are different, which may contribute to the slight differences in their antibacterial effect. Gram-positive bacteria were reported to be generally more susceptible to the anthocyanin action than Gram-negative ones (Cisowska, Wojnicz, & Hendrich, 2011). However, without elucidation of the antibacterial mechanisms, the antibacterial effect of the investigated compound is still unclear. Thus, *S. aureus* ATCC 25923 and *E. coli* ATCC 25922 were used in the succeeding studies to reveal the antibacterial mechanisms of C3G–LA against the aforementioned bacteria.

3.3 C3G–LA treatment inhibited the growth of *S. aureus* and *E. coli*

Different concentrations of C3G and C3G–LA were applied to *S. aureus* ATCC 25923 and *E. coli* ATCC 25922 to investigate the influence of these compounds on the viability of the two strains. As shown in Fig. 1, the treatment concentration of 1/2× MIC of either C3G or C3G–LA hardly influenced the growth of *S. aureus* and *E. coli*. However, the growth of both strains was inhibited by C3G treatment at the MIC and 2× MIC concentrations (Fig. 1**)**. The C3G–LA treatment at the MIC and 2× MIC concentrations also inhibited *E. coli* growth (Fig. 1B**)**. Interestingly, the treatment of C3G–LA at the level of 2× MIC sharply decreased the bacterial concentration of *S. aureus*, which reached 0 CFU/mL at 12 h (Fig. 1D), indicating the bactericidal effect of C3G–LA on *S. aureus*. Pagliarulo et al. (2016) reported similar bactericidal effects of polyphenol extracts from pomegranate crude juice against *S. aureus* but with a comparably high concentration of 160 mg/mL. The bactericidal ability of C3G–LA at a low concentration of 0.625 mg/mL against the most prevalent foodborne pathogen *S. aureus*, as determined in the present study, brings forth important application prospects for acylated anthocyanins in the food industry. Further investigation using real food to control such pathogens and associated diseases is anticipated.

3.4 C3G–LA disrupted cell membrane integrity

The LIVE/DEAD *Bac*Light Kit is composed of two nucleic acid-binding stains: SYTO 9TM and PI. SYTO 9TM penetrates all bacterial membranes and stains the cells as green, whilst PI only penetrates the cells with damaged membranes. The combination of the two stains produces red fluorescent cells. Thus, this scheme can be used to evaluate the integrity of cell membranes influenced by the exposure to exogenous substances (Zhao, Zhao, Phey, & Yang, 2019).

The cells treated with C3G and C3G–LA demonstrated an obvious impairment of cell membranes, as evidenced by the noticeable decreases in fluorescence intensity at 530 nm (Fig. 2). C3G–LA manifested stronger destructive power on *E. coli* and *S. aureu*s strains than C3G (Fig. 2). The application of 0.3125 mg/mL C3G–LA on the *S. aureus* 25923 strain decreased the fluorescence intensity by 96.2%, whilst the treatment of 10 mg/mL C3G could only reduce it by 75.0% (Fig. 2C and D). As for the *E. coli* 25922 strain, when C3G–LA was applied at 2.5, 5 and 10 mg/mL concentrations, the fluorescence intensity decreased significantly by 73.5%, 91.9% and 99.3%, respectively ($P < 0.01$, Fig. 2B). By contrast, only treatments with 5 and 10 mg/mL C3G concentrations induced significant reductions (by 52.4% and 97.9%, respectively, $P < 0.01$) in the fluorescence intensity plot (Fig. 2A).

The cell membrane acts as a barrier between the cytoplasm and the extracellular medium and thus is essential for maintaining the optimal internal conditions of cells for metabolism and energy transduction (Chen, Liu, Zhao, Zhang, Pang, & Yang, 2022; Sánchez, García & Heredia, 2010). Many researchers have suggested that phenolic compounds targeted the cytoplasmic membrane by accumulating hydrophobic phenolic groups in the lipid bilayer (Shi et al., 2016). They disrupt the lipid–protein interactions; alter the structure, function and permeability of cell membranes; accelerate the leakage of cell contents; disrupt the proton-motive force and electron influx and finally, destroy the integrity of cells (Araya-Cloutier, Vincken, van Ederen, den Besten, & Gruppen, 2018). In the present study, the introduction of fatty acid moiety to C3G could greatly increase the lipophilicity of the compound (Yang et al., 2019) and may result in the disruption of cell membranes.

3.5 C3G–LA treatment decreased intracellular ATP concentrations

As mentioned previously, C3G–LA exhibited strong destructive effects on the cell membranes of *E. coli* and *S. aureu*s. When the cell membrane was impaired, the intracellular ATP was decreased as a result of the decreased synthesis and increased hydrolysis of the ATP and the loss of inorganic phosphate through the highly compromised permeable cell membrane (He, Zhao, Chen, Zhao, & Yang, 2021). In the current study, the concentration of intracellular ATP displayed a gradual decreasing trend (Fig. 3) in response to the increased treatment level of C3G from 1/2× MIC (2.5 mg/mL) to 2× MIC (10 mg/mL). The ATP content was attenuated by 19%, 67% and 83% in *E. coli* 25922 and by 6%, 29% and 43% in *S. aureus* 25923 at the C3G treatment levels of 1/2× MIC, MIC and 2× MIC (in accordance with 2.5, 5 and 10 mg/mL), respectively (Fig. 3A and C). By contrast, the ATP content was sharply decreased at the lowest concentrations (1/2× MIC, 2.5 mg/mL for *E. coli* and 0.156 mg/mL for *S. aureus*) of the applied C3G–LA treatment. The ATP concentration was reduced by 88%, 92% and 94% in *E. coli* 25922 when the cells were treated with 2.5, 5 and 10 mg/mL of C3G–LA, respectively (P < 0.0001, Fig. 3B). When the *S. aureus* cells were treated with C3G–LA at the concentration of 0.156 mg/mL (1/2× MIC), the intracellular ATP level decreased extensively by 90% (P < 0.0001). The further increase in C3G–LA treatment concentration to 0.625 mg/mL (2× MIC) resulted in a reduction by 99% compared with that of the control (Fig. 3D). ATP is essential for many cell functions, including substance transportation across cell membranes (Shi et al., 2016). The loss of K^+ and H^+ ions and the failure of respiration could lead to detrimental effects on cell energy generation (Chang et al., 2021). Thus, the vast depletion of the intracellular ATP pool resulting from C3G–LA treatment could help explain the extensive disruption of cell viability.

3.6 C3G–LA treatment reduced intracellular pH

pH_{in} is critical in controlling various crucial cellular processes, such as DNA transcription, protein synthesis and enzyme activity, and it is considered an important indicator of bacterial cell damage (Yang et al., 2021). The integrity of cell membranes ensures the maintenance of pH_{in} via well-functioning ion channels in the presence of a moderate change of extracellular pH (Chang et al., 2021). Thus, the impairment of cell membranes in response to C3G–LA exposure may disturb the internal pH of bacterial cells. The pH_{in} values of the cells under different treatments of C3G and C3G–LA were evaluated (Fig. 4). The application of C3G and C3G–LA decreased the pH_{in} in *E. coli* 25922 and *S. aureus* 25923. The pH_{in} values of the normal *E. coli* 25922 and *S. aureus* 25923 were 7.25

and 7.75, respectively. When C3G was applied at 1/2× MIC, MIC and 2× MIC, the pH_{in} values of *E. coli* 25922 decreased from 7.25 to 6.82, 6.75 and 6.48, respectively (Fig. 4A), accounting for 6%, 7% and 11% of the reduction, respectively. The application of C3G–LA at 1/2× MIC, MIC and 2× MIC resulted in 1%, 9% and 12% reduction in the pH_{in} of *E. coli* 25922, i.e. from 7.25 to 7.15, 6.61 and 6.38, respectively (Fig. 4B). For the *S. aureus* 25923 cells, the presence of C3G at 1/2× MIC, MIC and 2× MIC reduced the pH_{in} by 12%, 13% and 28%, i.e. from 7.75 to 6.80, 6.73 and 5.56, respectively (Fig. 4C). The C3G–LA applied at the concentration of 1/2× MIC on *S. aureus* 25923 cells did not lead to any fluctuation in pH_{in} but the application of MIC and 2× MIC of C3G–LA reduced the pH_{in} by 11% and 16% (Fig. 4D), respectively. However, in consideration of the administration levels, C3G–LA exhibited a much stronger effect on pH_{in} in *S. aureus* 25923.

3.7 C3G–LA treatment destroyed cell membrane structure

The FESEM results (Fig. 5) indicated a destruction of the cell membrane structure by C3G–LA at the lower concentrations compared with that by C3G. Figs. 5A, E, I and M show normal cells with smooth surfaces and complete structures, whereas the other subfigures of cells treated with C3G and C3G–LA show disrupted membranes and deformed cell walls. The cell surface started to shrink to different degrees when treated with different levels of C3G and C3G–LA. The percentage of damaged cells and the degree of damage increased as the concentration of C3G and C3G–LA increased. The microstructural observations were in accordance with the findings on the impaired cell membrane integrity, decreased intracellular ATP concentration and reduced pH_{in} under the application of C3G and C3G–LA, as observed in this study.

The enzymatic acylation of anthocyanins has been widely investigated and successfully achieved in the last decades. The aim of researchers was to improve the lipophilicity and stability of anthocyanins and extend their application. Regarding the limited information on the application properties of the newly derived anthocyanin–fatty acid esters, this study evaluated the antimicrobial potential of C3G–LA against two presentative foodborne bacteria, namely, *E. coli* and *S. aureus*. C3G–LA treatment attained excellent antibacterial activity against *S. aureus,* with MIC of 0.3125 mg/mL compared with 5 mg/mL of its precursor (C3G). It effectively inhibited the growth of *S. aureus* by disrupting the cell membrane. The inhibition was evidenced by the damage of the membrane structure, the decrease in intracellular ATP concentrations and the changes in pH_{in} under C3G–LA treatments. The findings indicated the bactericidal potential of C3G–LA against *S. aureus* as it could fully kill bacteria under the 0.625 mg/mL treatment level. However, the antibacterial activity of C3G–LA was only comparably modest with respect to that of C3G against *E. coli,* with MIC of 5 mg/mL for both compounds. The findings of this research suggested that C3G–LA could be adopted as an alternative food preservative or a therapeutic agent against foodborne pathogens, especially *S. aureus*. Thus, evaluating the application of acylated anthocyanin in real food matrix is suggested (Wang, Wu, & Yang, 2022). More investigations could also be conducted for further elucidation of its preservative mechanisms through more state-of-the-art methods and techniques, such as NMR spectroscopic analysis (Wang, Wu, & Yang, 2022; He et al., 2021).

Supporting Information

Figure S1. Standard curves. A, Green fluorescence intensity at 530 nm and the percentage of viable bacteria of *E. coli* 25922; B, Green fluorescence intensity at 530 nm and the percentage of viable bacteria of *S. aureus* 25923.

Figure S2. Standard curve of ATP standards.

AUTHOR INFORMATION

Corresponding Author

*Zheng J, Tel: +86-18148962369; E-mail: zhengjie@jnu.edu.cn

ORCID

Jie Zheng: 0000-0001-9755-5595

Funding

This work was supported by the Guangzhou Science Technology and Innovation Commission (201904010400), National Natural Science Foundation of China (32001796), the Innovation Center Project by Zhongshan Torch Modern Industrial Engineering and Technology Research Institute (2019CYY01002), the Pearl River Talent Program (2017GC010360) by Guangdong Science and Technology Department, Guangzhou Science and Technology Planning Project (202002030145), and the Foundation for Research of Natural Resources in Finland (2018001).

Conflict of interest

The authors declare no competing financial interest.

Reference

Abebe, E., Gugsa, G., & Ahmed, M. (2020). Review on major food-borne zoonotic bacterial pathogens. *Journal of tropical medicine*, *2020*, 4674235.

Alakomi, H. L., Mättö, J., Virkajärvi, I., & Saarela, M. (2005). Application of a microplate scale fluorochrome staining assay for the assessment of viability of probiotic preparations. *Journal of Microbiological Methods*, *62*(1), 25–35.

Aloud, B. M., Petkau, J. C., Yu, L., McCallum, J., Kirby, C., Netticadan, T., & Blewett, H. (2020). Effects of cyanidin 3-O-glucoside and hydrochlorothiazide on T-cell phenotypes and function in spontaneously hypertensive rats. *Food & Function*, *11*(10), 8560.

Araya-Cloutier, C., Vincken, J. P., van Ederen, R., den Besten, H. M., & Gruppen, H. (2018). Rapid membrane permeabilization of *Listeria monocytogenes* and *Escherichia coli* induced by antibacterial prenylated phenolic compounds from legumes. *Food Chemistry*, *240*, 147-155.Breeuwer, P., Drocourt, J., Rombouts, F. M., & Abee, T. (1996). A Novel method for continuous determination of the intracellular pH in bacteria with the internally conjugated fluorescent probe 5 (and 6-)-carboxyfluorescein succinimidyl ester. *Applied and Environmental Microbiology*, *62*(1), 178-183.

Chang, Y., Xing, M., Hu, X., Feng, H., Wang, Y., Guo, B., Sun, M., Ma, L., & Fei, P. (2021). Antibacterial activity of *Chrysanthemum buds* crude extract against *Cronobacter sakazakii* and its application as a natural disinfectant. *Frontiers in Microbiology*, *11*, 632177.

Chen, L., Liu, Q., Zhao, X., Zhang, H., Pang, X., & Yang, H. (2022). Inactivation efficacies of lactic acid and mild heat treatments against *Escherichia coli* strains in organic broccoli sprouts. *Food Control*, *133*, 108577.

Chen, K., Wei, X., Zhang, J., Pariyani, R., Jokioja, J., Kortesniemi, M., Linderborg, K. M., Heinonen, J., Sainio, T., Zhang, Y., & Yang, B. (2020). Effects of anthocyanin extracts from bilberry (*Vaccinium myrtillus L.*) and purple potato (*Solanum tuberosum L*. var. 'Synkea Sakari') on the plasma metabolomic profile of zucker diabetic fatty rats. *Journal of Agricultural and Food Chemistry*, *68*(35), 9436–9450.

Chen, S., Zhou, H., Zhang, G., Meng, J., Deng, K., Zhou, W., Wang, H., Wang, Z., Hu, N., & Suo, Y. (2019). Anthocyanins from *Lycium ruthenicum Murr.* Ameliorated d-galactose-induced memory impairment, oxidative stress, and neuroinflammation in adult rats. *Journal of Agricultural and Food Chemistry*, *67*(11), 3140–3149.

Cisowska, A., Wojnicz, D., & Hendrich, A. B. (2011). Anthocyanins as antimicrobial agents of natural plant origin. *Natural product communications*, *6*(1), 1934578X1100600136.

CLSI. (2017). Performance Standards for Antimicrobial Susceptibility Testing. Wayne, PA.

Cruz, L., Guimarães, M., Araújo, P., Évora, A., de Freitas, V., & Mateus, N. (2017). Malvidin 3-glucoside–fatty acid conjugates: from hydrophilic toward novel lipophilic derivatives. *Journal of Agricultural and Food Chemistry*, *65*(31), 6513-6518.

Khalil, I. A., Troeger, C., Blacker, B. F., Rao, P. C., Brown, A., Atherly, D. E., Brewer, T. G., Engmann, C. M., Houpt, E. R., Kang, G., Kotloff, K. L., Levine, M. M., Luby, S. P., MacLennan, C. A., Pan, W. K., Pavlinac, P. B., Platts-Mills, J. A., Qadri, F., Riddle, M. S., Ryan, E. T., Shoultz, D. A., Steele, A. D., Walson, J. L., Sanders, J. W., Mokdad,

A. H., Murray, C. J. L., Hay, S. I., & Reiner Jr, R. C. (2018). Morbidity and mortality due to shigella and enterotoxigenic *Escherichia coli* diarrhoea: the Global Burden of Disease Study 1990–2016. *The Lancet infectious diseases*, *18*(11), 1229-1240.

Gong, S., Fei, P., Sun, Q., Guo, L., Jiang, L., Duo, K., Bi, X., & Yun, X. (2021). Action mode of cranberry anthocyanin on physiological and morphological properties of *Staphylococcus aureus* and its application in cooked meat. *Food Microbiology*, *94*, 103632.

Guimarães, M., Mateus, N., de Freitas, V., & Cruz, L. (2018). Improvement of the color stability of cyanidin-3-glucoside by fatty acid enzymatic acylation. *Journal of Agricultural and Food Chemistry*, *66*(38), 10003–10010.

He, Y., Zhao, X., Chen, L., Zhao, L., & Yang, H. (2021). Effect of electrolysed water generated by sodium chloride combined with sodium bicarbonate solution against *Listeria innocua* in broth and on shrimp. *Food Control*, *127*, 108134

Jang, J., Hur, H. G., Sadowsky, M. J., Byappanahalli, M. N., Yan, T., & Ishii, S. (2017). Environmental *Escherichia coli*: ecology and public health implications—a review. *Journal of Applied Microbiology*, *123*(3), 570-581.

Jiang, C., Sun, Z. M., Hu, J. N., Jin, Y., Guo, Q., Xu, J. J., Chen, Z. X., Jiang, R. H., & Wu, Y. S. (2019). Cyanidin ameliorates the progression of osteoarthritis via the Sirt6/NF-κB axis in vitro and in vivo. *Food & Function*, *10*(9), 5873.

Jugran, A. K., Rawat, S., Devkota, H. P., Bhatt, I. D., & Rawal, R. S. (2021). Diabetes and plant- derived natural products: From ethnopharmacological approaches to their potential for modern drug discovery and development. *Phytotherapy Research*, *35*(1), 223-245.

Krga, I., & Milenkovic, D. (2019). Anthocyanins: from sources and bioavailability to cardiovascular-health benefits and molecular mechanisms of action. *Journal of Agricultural and Food Chemistry*, *67*(7), 1771–1783.

Laupland, K. B., Steele, L., Pasquill, K., & Parfitt, E. C. (2021). *Staphylococcus aureus* bloodstream infection: Secular changes associated with the implementation of a de novo clinical infectious diseases service in a Canadian population. *International Journal of Infectious Diseases*, *104*, 45-49.

Li, G., Wang, X., Xu, Y., Zhang, B., & Xia, X. (2014). Antimicrobial effect and mode of action of chlorogenic acid on *Staphylococcus aureus*. *European food research and technology*, *238*(4), 589-596.

Liu, F., Zhao, F., Wang, W., Sang, J., Jia, L., Li, L., & Lu, F. (2020). Cyanidin-3-O-glucoside inhibits Aβ40 fibrillogenesis, disintegrates preformed fibrils, and reduces amyloid cytotoxicity. *Food & Function, 11*(3), 2573.

Ma, Y., Ding, S., Fei, Y., Liu, G., Jang, H., & Fang, J. (2019). Antimicrobial activity of anthocyanins and catechins against foodborne pathogens *Escherichia coli* and *Salmonella*. *Food Control*, *106*, 106712.

Marquez-Rodriguez, A. S., Guimarães, M., Mateus, N., de Freitas, V., Ballinas-Casarrubias, M. L., Fuentes-Montero, M. E., Salas, E., & Cruz, L. (2021). Disaccharide anthocyanin delphinidin 3-O-sambubioside from *Hibiscus sabdariffa L.*: Candida antarctica lipase B-catalyzed fatty acid acylation and study of its color properties. *Food Chemistry*, *344*, 12860.

Oliveira, H., Correia, P., Bessa, L. J., Guimares, M., & Fernandes, I. (2021). Cyanidin-3-glucoside lipophilic conjugates for topical application: tuning the antimicrobial activities with fatty acid chain length. *Processes*, *9*(2), 340.

Pagliarulo, C., De Vito, V., Picariello, G., Colicchio, R., Pastore, G., Salvatore, P., & Volpe, M. G. (2016). Inhibitory effect of pomegranate (*Punica granatum L.*) polyphenol extracts on the bacterial growth and survival of clinical isolates of pathogenic *Staphylococcus aureus* and *Escherichia coli*. *Food Chemistry*, *190*, 824-831.

Pertuzatti, P. B., Barcia, M. T., Portugal, L., Rebello, G., & Hermosín-Gutiérrez, I. (2016). Antimicrobial activity and differentiation of anthocyanin profiles of rabbiteye and highbush blueberries using HPLC–DAD–ESI-MSn and multivariate analysis. *Journal of Functional Foods*, *26*, 506-516.

Ronco, T., Jørgensen, N. S., Holmer, I., Kromann, S., Sheikhsamani, E., Permin, A., Svenningsen, S. W., Christensen, J. B., & Olsen, R. H. (2020). A novel promazine derivative shows high in vitro and in vivo antimicrobial activity against *Staphylococcus aureus*. *Frontiers in Microbiology*, *11*, 560798.

Sánchez, E., García, S., & Heredia, N. (2010). Extracts of edible and medicinal plants damage membranes of *Vibrio cholera*. *Applied and Environmental Microbiology*, *76*(20), 6888–6894.

Sarowska, J., Futoma-Koloch, B., Jama-Kmiecik, A., Frej-Madrzak, M., Ksiazczyk, M., Bugla-Ploskonska, G., & Choroszy-Krol, I. (2019). Virulence factors, prevalence and potential transmission of extraintestinal pathogenic *Escherichia coli* isolated from different sources: recent reports. *Gut Pathogens*, *11*(1), 1-16.

Shi, C., Sun, Y., Zheng, Z., Zhang, X., Song, K., Jia, Z., Chen, Y., Yang, M., Liu, X., Dong, R., & Xia, X. (2016). Antimicrobial activity of syringic acid against *Cronobacter sakazakii* and its effect on cell membrane. *Food Chemistry*, *197*, 100–106.

Tong, S. Y., Davis, J. S., Eichenberger, E., Holland, T. L., & Fowler, V. G. Jr. (2015). *Staphylococcus aureus* infections: epidemiology, pathophysiology, clinical manifestations, and management. *Clinical Microbiology Reviews*, *28*(3), 603-661.

Wang, Y., Wu, J. E., & Yang, H. (2022). Comparison of the metabolic responses of eight *Escherichia coli* strains including the “big six” in pea sprouts to low concentration electrolysed water by NMR spectroscopy. *Food Control*, *131*, 108458.

Wang, Y., Lin, J., Tian, J., Si, X., Jiao, X., Zhang, W., Gong, E., & Li, B. (2019). Blueberry Malvidin-3-galactoside suppresses hepatocellular carcinoma by regulating apoptosis, proliferation, and metastasis pathways in vivo and in vitro. *Journal of Agricultural and Food Chemistry*, *67*(2), 625–636.

Wei, J., Zhang, G., Zhang, X., Xu, D., Gao, J., Fan, J., & Zhou, Z. (2017). Anthocyanins from black chokeberry (*Aroniamelanocarpa Elliot*) delayed aging-related degenerative changes of brain. *Journal of Agricultural and Food Chemistry*, *65*(29), 5973–5984.

Yang, W., Kortesniemi, M., Ma, X., Zheng, J., & Yang, B. (2019). Enzymatic acylation of blackcurrant (*Ribes nigrum*) anthocyanins and evaluation of lipophilic properties and antioxidant capacity of derivatives. *Food Chemistry*, *281*,189-196.

Yang, W., Kortesniemi, M., Yang, B., & Zheng, J. (2018). Enzymatic acylation of anthocyanins isolated from Alpine bearberry (*Arctostaphylos alpina*) and lipophilic properties, thermostability, and antioxidant capacity of the derivatives. *Journal of Agricultural and Food Chemistry*, *66*(11), 2909−2916.

Yang, X., Sun, H., Tu, L., Jin, Y., Wang, M., Liu, S., Zhang, Z., & He, S. (2020a). Investigation of acute, subacute and subchronic toxicities of anthocyanin derived acylation reaction products and evaluation of their antioxidant activities in vitro. *Food & Function*, *11*(12), 10954-10967.

Yang, X., Sun, H., Tu, L., Jin, Y., Zhang, Z., Wang, M., Liu, S., Wang, Y., & He, S. (2020b). Kinetics of enzymatic synthesis of cyanidin-3-glucoside lauryl ester and its physicochemical property and proliferative effect on intestinal probiotics. *Biology*, *9*(8), 205.

Li, G. H., Wang, X., Xu, Y. F., Zhang, B. G., & Xia, X. D. (2014). Antimicrobial effect and mode of action of chlorogenic acid on *Staphylococcus aureus*. *European Food Research and Technology*, 238, 589–596.

Zhang, P., Liu, S., Zhao, Z., You, L., Harrison, M. D., & Zhang, Z. (2021). Enzymatic acylation of cyanidin-3-glucoside with fatty acid methyl esters improves stability and antioxidant activity. *Food Chemistry*, *343*, 128482

Zhao, L., Zhao, M. Y., Phey, C. P., & Yang, H. (2019). Efficacy of low concentration acidic electrolysed water and levulinic acid combination on fresh organic lettuce (*Lactuca sativa Var. Crispa L.*) and its antimicrobial mechanism. *Food Control*, *101*, 241-250.

Zhou, P., Huang, C., Liu, F., Bai, W., Ou, S., & Zheng, J. (2021). Preparation and stability analysis of anthocyanin from black bean hull by enzymatic acylation. *Fine Chemicals*, *38*(7), 1416-1422.

Figure captions

Figure 1. Growth curves of *E. coli* ATCC 25922 and *S. aureus* ATCC 25923 treated with different concentrations of C3G and C3G–LA. A and B, *E. coli* ATCC 25922 treated with C3G and C3G–LA, respectively. C and D, *S. aureus* ATCC 25923 treated with C3G and C3G–LA, respectively.

Figure 2. Effects of different C3G and C3G–LA concentrations on the membrane integrity of *E. coli* 25922 and *S. aureus* 25923. A and B, *E. coli* 25922 treated with C3G and C3G–LA, respectively. C and D, *S. aureus* 25923 treated with C3G and C3G–LA, respectively. Significant differences from the control group (0 mg/mL) represented by ** (P < 0.01), *** (P < 0.001) and **** (P < 0.0001).

Figure 3. Effects of different C3G and C3G–LA concentrations on the content of intracellular ATP in bacterial cells. A and B, *E. coli* 25922 treated with C3G and C3G–LA, respectively. C and D, *S. aureus* 25923 treated with C3G and C3G–LA, respectively. Significant differences from the control group (0 mg/mL) represented by * (P < 0.05), *** (P < 0.001) and **** (P < 0.0001).

Figure 4. Effects of different C3G and C3G–LA concentrations on the pH_{in} of *E. coli* 25922 (A and B for C3G and C3G–LA, respectively) and *S. aureus* 25923 (C and D for C3G and C3G–LA, respectively). pH_{in} values in the solid lines calculated from the ratios of fluorescence emission intensity at 490 nm and 440 nm. Significant differences from the control group (0 mg/mL) represented by * (P < 0.05), ** (P < 0.01), *** (P < 0.001) and **** (P < 0.0001).

Figure 5. FESEM analyses of *E. coli* 25922 and *S. aureus* 25923 treated with different C3G and C3G–LA concentrations. A, B, C and D, *E. coli* 25922 treated with 0 mg/mL,

1/2×MIC, MIC and 2×MIC of C3G, respectively. E, F, G and H, *E. coli* 25922 treated with 0 mg/mL, 1/2×MIC, MIC and 2×MIC of C3G–LA, respectively. I, J, K and L, *S. aureus* 25923 treated with 0 mg/mL, 1/2×MIC, MIC and 2×MIC of C3G, respectively. M, N, O and P, *S. aureus* 25923 treated with 0 mg/mL, 1/2×MIC, MIC and 2×MIC of C3G–LA, respectively.

Table 1. MIC values of C3G and C3G–LA on different strains.

Strains	Origin	MIC (mg/mL)[a]	
		C3G	C3G–LA
S. aureus ATCC 25923		5	0.3125
S. aureus SJS001	Chicken	5	0.3125
S. aureus SJS008	Chicken	5	0.3125
S. aureus SJS009	Pork	5	0.3125
S. aureus SJS010	Pork	5	0.3125
E. coli ATCC 25922		5	5
E. coli QD016	Duck	5	5
E. coli QD021	Duck	5	5
E. coli QD023	Chicken	5	5
E. coli QD025	Chicken	5	5

[a] MIC, minimum inhibitory concentration; C3G, cyanidin-3-*O*-glucoside; C3G–LA, cyanidin-3-*O*-glucoside–lauric acid ester.

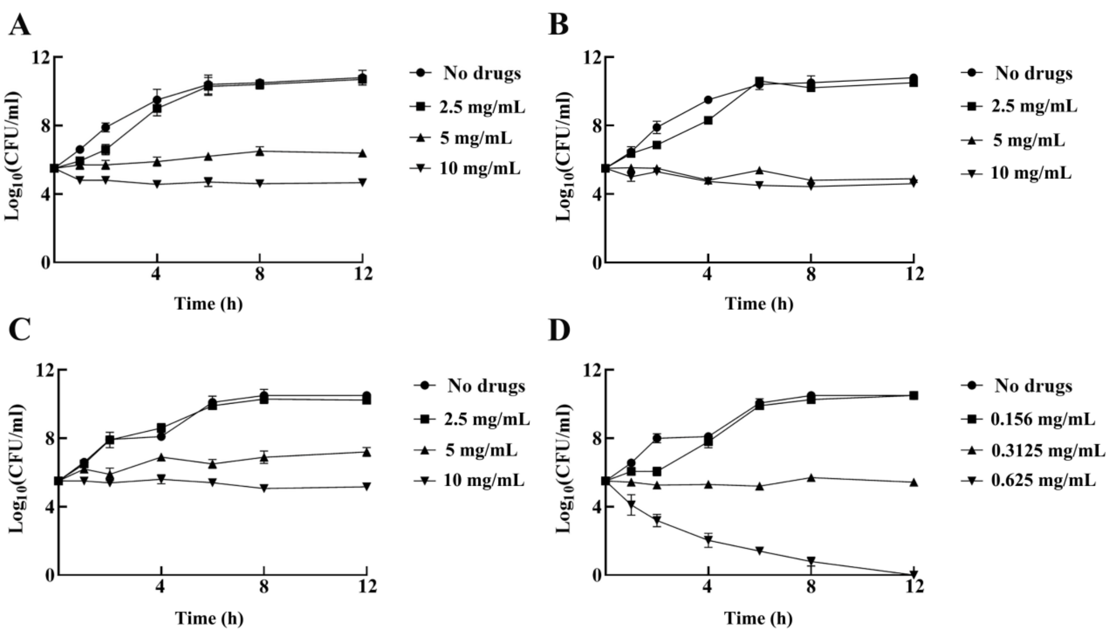
A
B
C
D
Log$_{10}$(CFU/ml)
Time (h)
No drugs
2.5 mg/mL
5 mg/mL
10 mg/mL
0.156 mg/mL
0.3125 mg/mL
0.625 mg/mL
0
4
8
12

Figure 1.

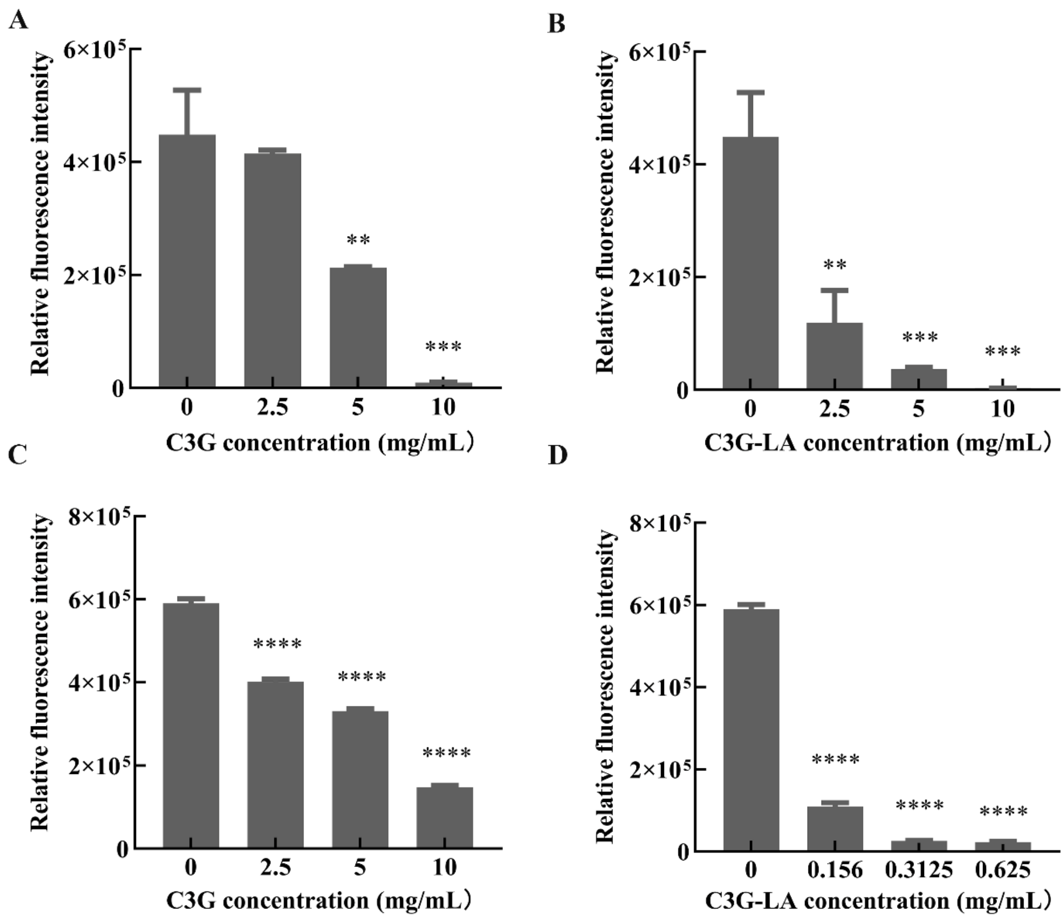
A
6×10⁵
4×10⁵
2×10⁵
0
Relative fluorescence intensity
**
***
0
2.5
5
10
C3G concentration (mg/mL)
B
6×10⁵
4×10⁵
2×10⁵
0
Relative fluorescence intensity
**
***
***
0
2.5
5
10
C3G-LA concentration (mg/mL)
C
8×10⁵
6×10⁵
4×10⁵
2×10⁵
0
Relative fluorescence intensity
****
****
****
0
2.5
5
10
C3G concentration (mg/mL)
D
8×10⁵
6×10⁵
4×10⁵
2×10⁵
0
Relative fluorescence intensity
****
****
****
0
0.156
0.3125
0.625
C3G-LA concentration (mg/mL)

Figure 2.

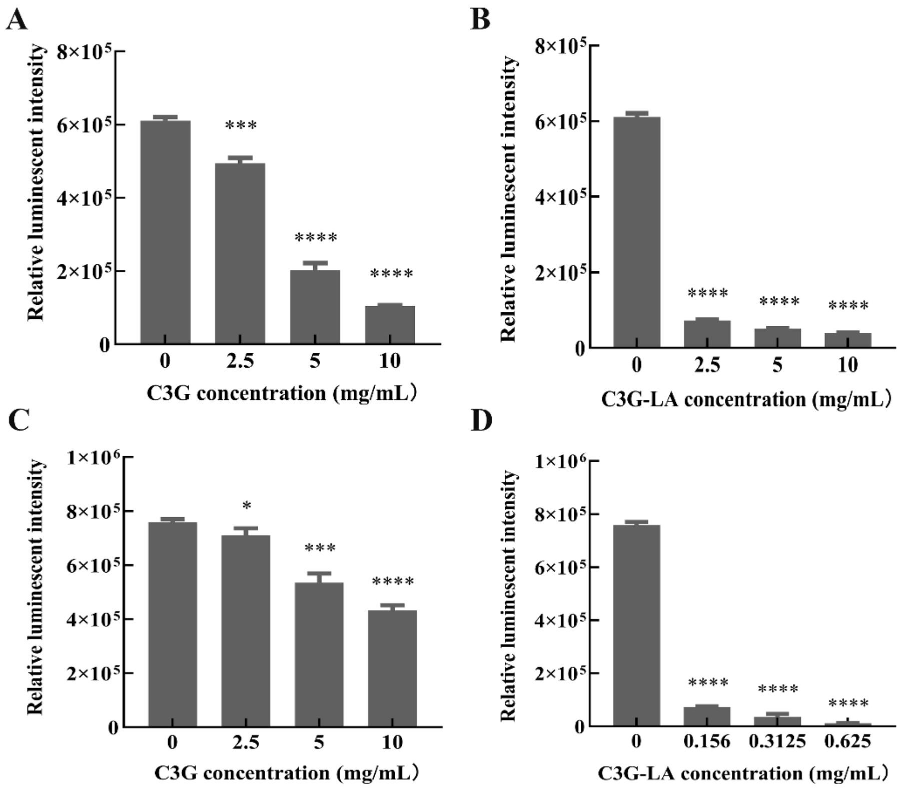
A
B
C
D
Relative luminescent intensity
8×10⁵
6×10⁵
4×10⁵
2×10⁵
1×10⁶
0
***
****
*
2.5
5
10
0.156
0.3125
0.625
C3G concentration (mg/mL)
C3G-LA concentration (mg/mL)

Figure 3.

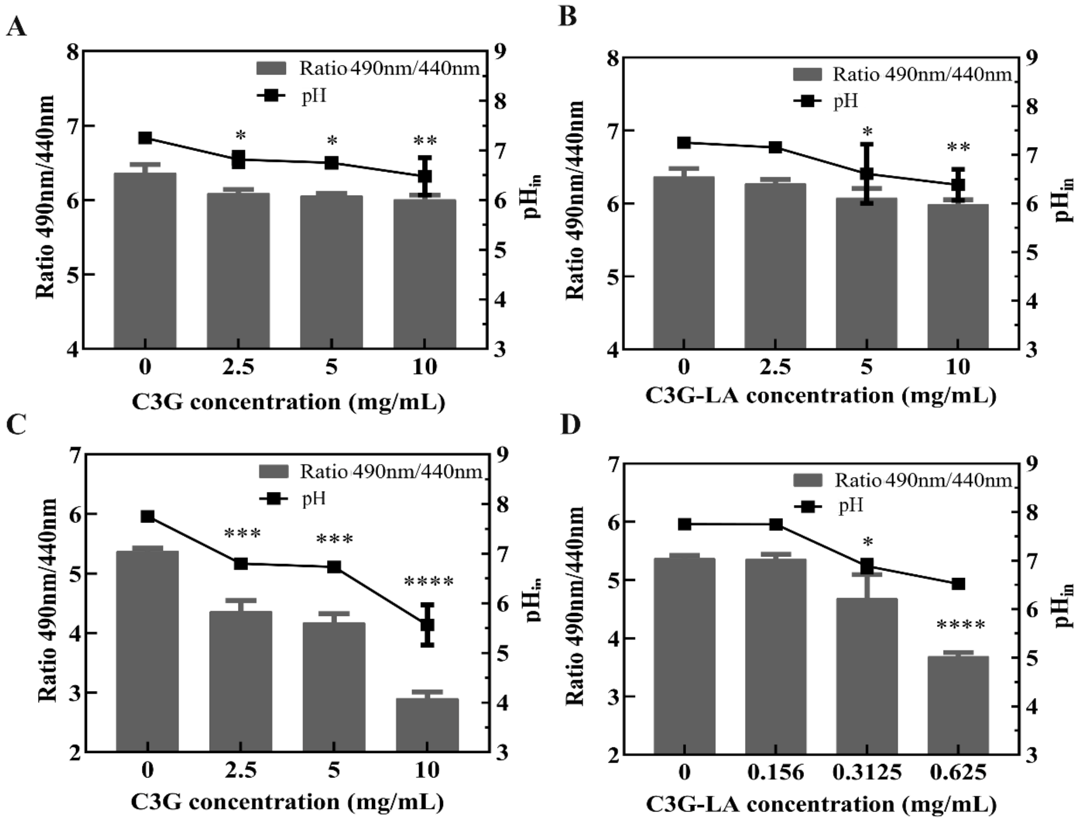
A
B
C
D
Ratio 490nm/440nm
pH
pH
Ratio 490nm/440nm
pHin
C3G concentration (mg/mL)
C3G-LA concentration (mg/mL)
0
2.5
5
10
0.156
0.3125
0.625

Figure 4.

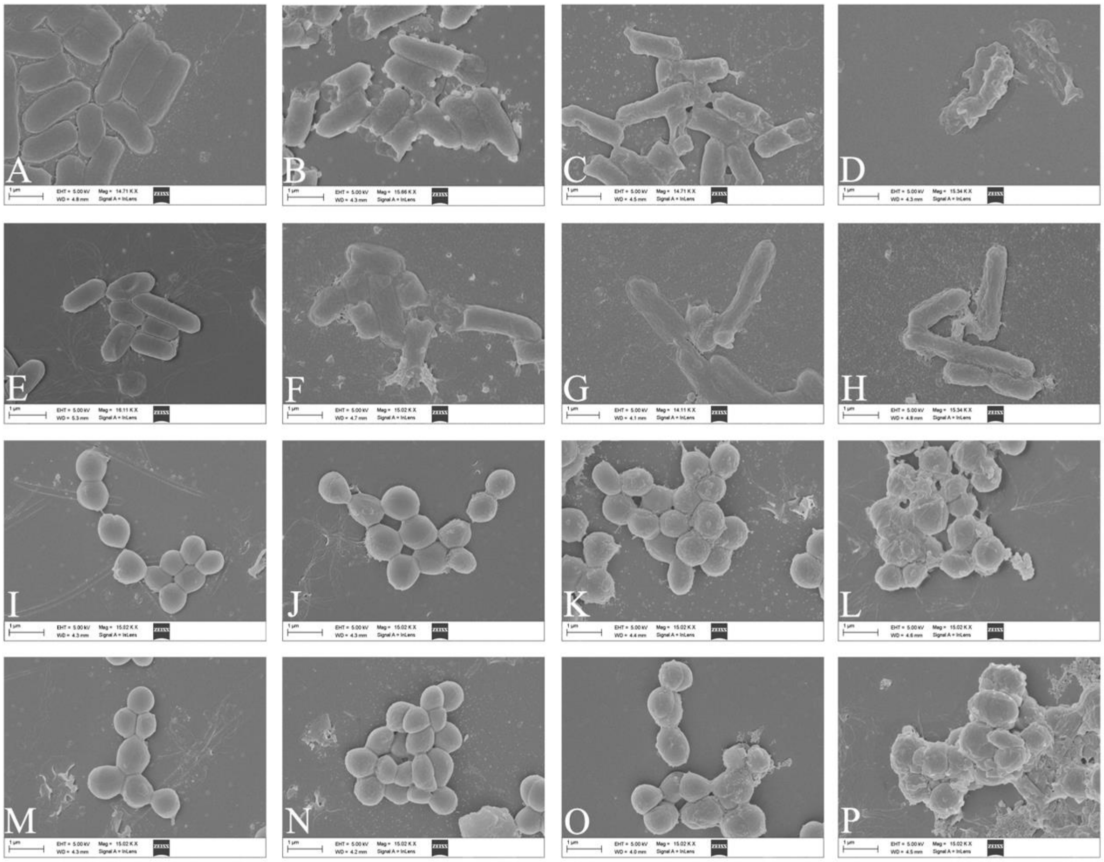

Figure 5.